

Supporting Information

Corrosion Control of Chrome Steel Ball in Nitric Acid Medium Using Schiff Base Ligand and Corresponding Metal Complexes: A Combined Experimental and Theoretical Study

Sourav Kr. Saha^{a,b}, Pritam Ghosh^a, Additi RoyChowdhury^{a,b}, Pranab Samanta^{a,b}, N. C. Murmu^a, Aditya Kr. Lohar^c and Priyabrata Banerjee^{a,b,*}

^aSurface Engineering & Tribology Group, CSIR-Central Mechanical Engineering Research Institute, Mahatma Gandhi Avenue, Durgapur 713209, West Bengal, India. Fax: +91-343-2546 745; Tel: +91-343-6452220.

^bAcademy of Scientific & Innovative Research, Anusandhan Bhawan, 2 Rafi Marg, New Delhi-110001, India.

^cFoundry Group, CSIR-Central Mechanical Engineering Research Institute, Mahatma Gandhi Avenue, Durgapur 713209, West Bengal, India

**Corresponding Author, E-mail: pr_banerjee@cmeri.res.in, priyabrata_banerjee@yahoo.co.in*

Table S1. Inhibition efficiency (% I.E.) calculated from weight loss technique on chrome steel surface in 0.1 N HNO₃ solutions without and with various concentration of the 2-(2-hydroxybenzylideneamino)phenol.

Inhibitor	Concentration (mM)	Reaction time (Hours)	Initial weight (gm)	Final weight (gm)	Loss in weight (gm)	Surface coverage (θ)	Inhibition efficiency (%)
HBAP	0.0	24	8.4090	8.3646	0.0444	–	–
	0.05	24	8.4132	8.3727	0.0405	0.0878	8.78
	0.075	24	8.4152	8.3757	0.0395	0.1104	11.04
	0.1	24	8.4115	8.3736	0.0379	0.1464	14.64
	0.2	24	8.4044	8.3713	0.0331	0.2545	25.45
	0.4	24	8.4256	8.3970	0.0286	0.3558	35.58

Table S2. Inhibition efficiency (% I.E.) calculated from weight loss technique on chrome steel surface in 0.1 N HNO₃ solutions without and with various concentration of the Mn-HBAP.

Inhibitor	Concentration (mM)	Reaction time (Hours)	Initial weight (gm)	Final weight (gm)	Loss in weight (gm)	Surface coverage (θ)	Inhibition efficiency (%)
Mn-HBAP	0.05	24	8.4129	8.3742	0.0387	0.1284	12.84
	0.075	24	8.3968	8.3589	0.0379	0.1464	14.64
	0.1	24	8.4031	8.3668	0.0363	0.1824	18.24
	0.2	24	8.4259	8.3947	0.0312	0.2973	29.73
	0.4	24	8.4098	8.3842	0.0256	0.4234	42.34

Table S3. Inhibition efficiency (% I.E.) calculated from weight loss technique on chrome steel surface in 0.1 N HNO₃ solutions without and with various concentration of the Co-HBAP.

Inhibitor	Concentration (mM)	Reaction time (Hours)	Initial weight (gm)	Final weight (gm)	Loss in weight (gm)	Surface coverage (θ)	Inhibition efficiency (%)
Co-HBAP	0.05	24	8.4187	8.3787	0.0400	0.0991	9.91
	0.075	24	8.4254	8.3863	0.0391	0.1194	11.94
	0.1	24	8.4025	8.3651	0.0374	0.1576	15.76
	0.2	24	8.4123	8.3795	0.0328	0.2613	26.13
	0.4	24	8.4267	8.3984	0.0283	0.3626	36.26

Table S4. Peaks and assignments of IR adsorption by HBAP and chrome steel corrosion product (containing HBAP as an inhibitor).

2-(2-hydroxybenzylideneamino)phenol		Corrosion product	
Peak (cm ⁻¹)	Assignments	Peak (cm ⁻¹)	Assignments
1461 cm ⁻¹	C-C stretch	1461 cm ⁻¹	C-C stretch
1630 cm ⁻¹	C=N stretch	1602 cm ⁻¹	C=N stretch
3042 cm ⁻¹	-C-H stretch	2927 cm ⁻¹	-C-H stretch

Table S5. Peaks and assignments of IR adsorption by Mn-HBAP and chrome steel corrosion product (containing Mn-HBAP as an inhibitor).

Mn-HBAP		Corrosion product	
Peak (cm ⁻¹)	Assignments	Peak (cm ⁻¹)	Assignments
1461 cm ⁻¹	C-C stretch	1382 cm ⁻¹	C-C stretch
1597 cm ⁻¹	C=N stretch	1602 cm ⁻¹	C=N stretch
2942 cm ⁻¹	-C-H stretch	2920 cm ⁻¹	-C-H stretch

Table S6. Peaks and assignments of IR adsorption by Co-HBAP and chrome steel corrosion product (containing Co-HBAP as an inhibitor).

Co-HBAP		Corrosion product	
Peak (cm ⁻¹)	Assignments	Peak (cm ⁻¹)	Assignments
1476 cm ⁻¹	C-C stretch	1461 cm ⁻¹	C-C stretch
1612 cm ⁻¹	C=N stretch	1624 cm ⁻¹	C=N stretch
2970 cm ⁻¹	-C-H stretch	2927 cm ⁻¹	-C-H stretch

Table S7. IR Peaks and assignments of IR adsorption by Ni-HBAP and chrome steel corrosion product (containing Ni-HBAP as an inhibitor).

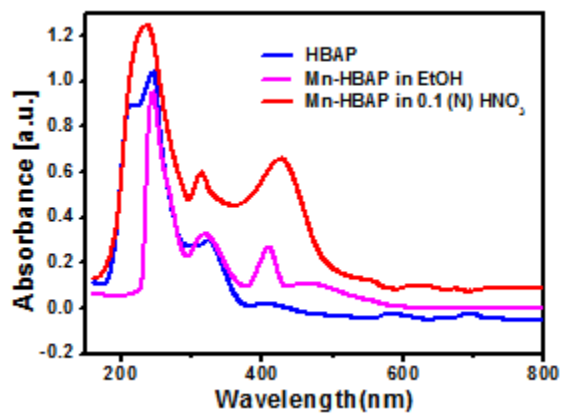
Ni-HBAP		Corrosion product	
Peak (cm ⁻¹)	Assignments	Peak (cm ⁻¹)	Assignments
1469 cm ⁻¹	C-C stretch	1454 cm ⁻¹	C-C stretch
1612 cm ⁻¹	C=N stretch	1623 cm ⁻¹	C=N stretch
2934 cm ⁻¹	-C-H stretch	2920 cm ⁻¹	-C-H stretch

Table S8. Description of three levels of factors with different metal-HBAP complexes as inhibitors.

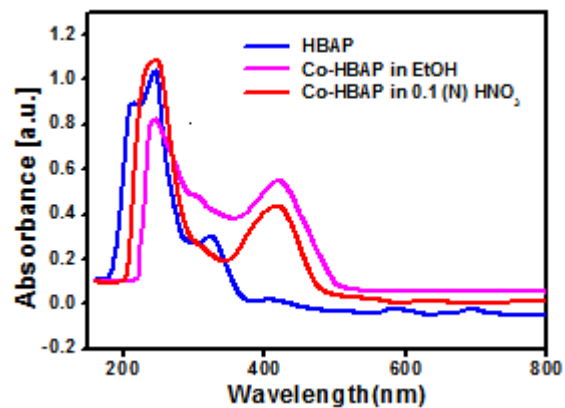
Name (Units)	Factors	Levels (Code Value)		
		Low (-1)	Mean (0)	High (1)
Composition/Comp	A	Co-HBAP	Mn-HBAP	Ni-HBAP
Concentration/Conc (mM)	B	0.05	0.1	0.15
Time(hr)	C	24	48	72

Table S9. Design table for DOE.

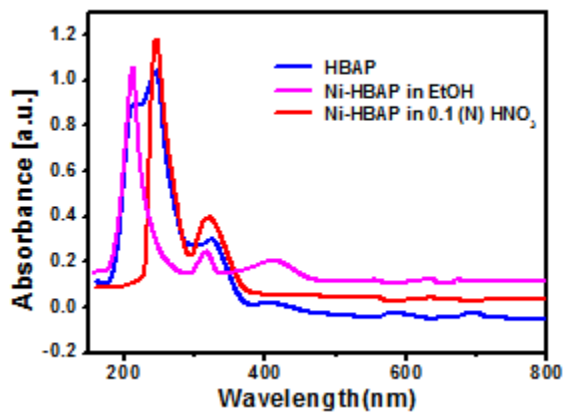
Std	Run	Factor A: Comp	Factor B: Conc (mM)	Factor C: Time (hr)	Efficiency (%)
12	1	Mn-HBAP	0.15	72	20.374
7	2	Co-HBAP	0.1	72	7.69
15	3	Mn-HBAP	0.1	48	14.04
11	4	Mn-HBAP	0.05	72	8.108
4	5	Ni-HBAP	0.15	24	12.997
8	6	Ni-HBAP	0.1	48	7.9
6	7	Ni-HBAP	0.1	24	19.36
1	8	Co-HBAP	0.05	48	6.289
9	9	Mn-HBAP	0.05	24	12.83
14	10	Mn-HBAP	0.1	48	12.99
17	11	Mn-HBAP	0.1	48	13.41
5	12	Co-HBAP	0.1	24	15.76
16	13	Mn-HBAP	0.1	48	13.83
13	14	Mn-HBAP	0.1	48	14.255
2	15	Ni-HBAP	0.05	48	5.66
10	16	Mn-HBAP	0.15	24	21.62
3	17	Co-HBAP	0.15	48	14.884



(a)



(b)



(c)

Figure S1. (a) UV-Visible absorption for HBAP and its corresponding Mn-complex in ethanol and in test solution (0.1 N HNO₃), (b) UV-Visible absorption for HBAP and its corresponding Co-complex in ethanol and in test solution and (c) UV-Visible absorption for HBAP and its corresponding Ni-complex in ethanol and in test solution.

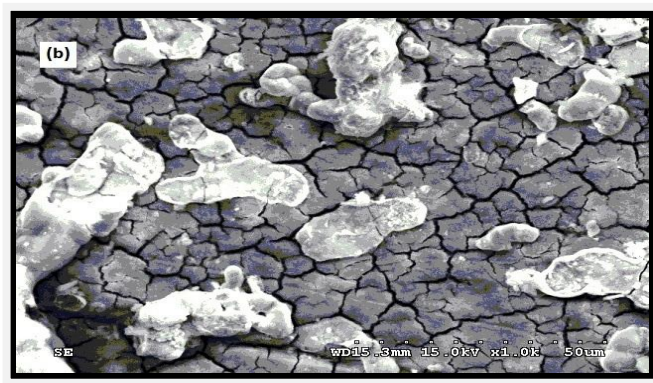


Figure S2. SEM micrograph of the chrome steel ball surfaces after immersion of 72 h in the presence of 0.1 mM 2-(2-hydroxybenzylideneamino)phenol in 0.1 N HNO₃.

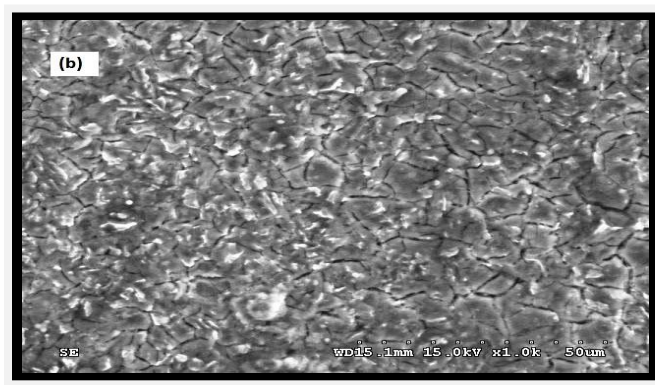
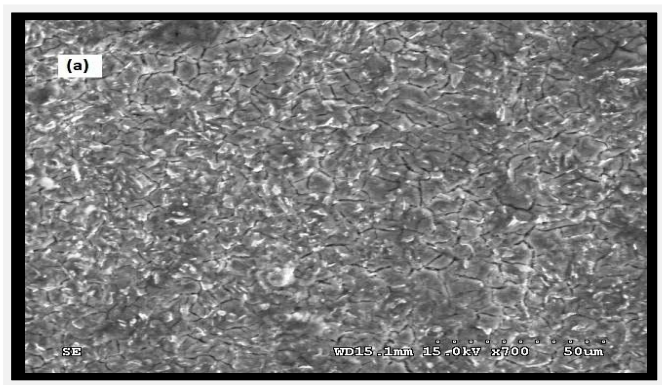


Figure S3. SEM micrograph of the chrome steel ball surfaces after immersion of 72 h in the presence of 0.05 mM of Mn-HBAP in 0.1 N HNO₃.

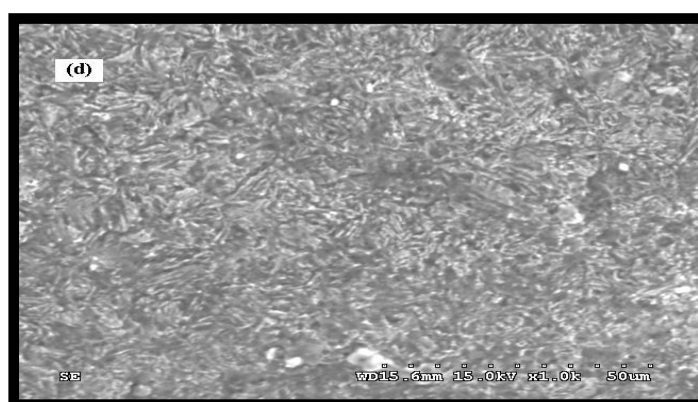
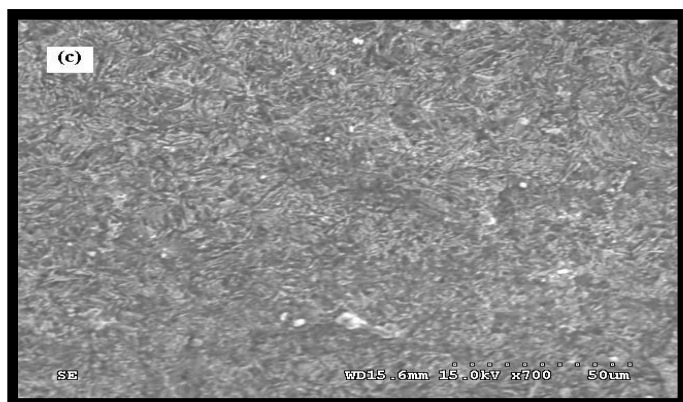


Figure S4. SEM micrograph of the chrome steel ball surfaces after immersion of 72 h in the presence of 0.1 mM of Co-HBAP in 0.1 N HNO₃.

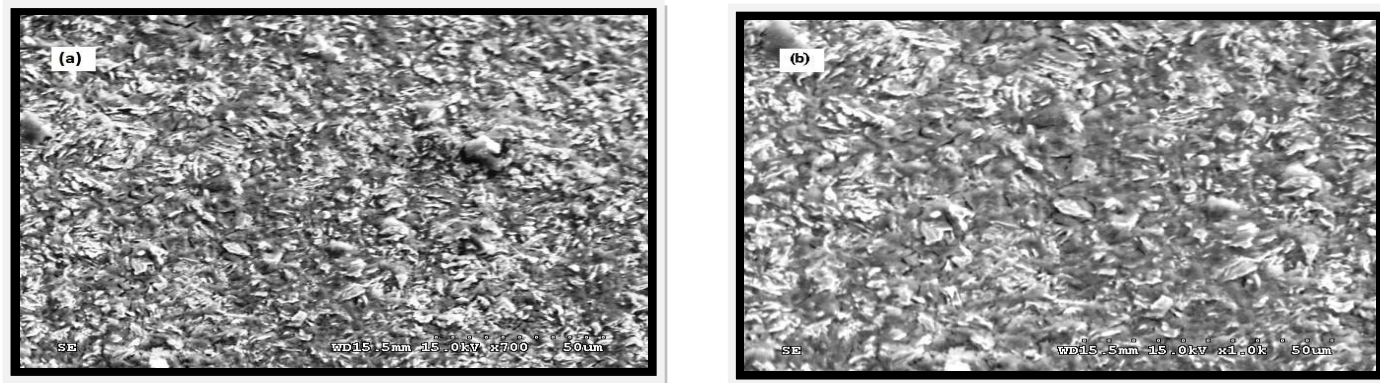


Figure S5. SEM micrograph of the chrome steel ball surfaces after immersion of 72 h in the presence of 0.1 mM of Ni-HBAP in 0.1 N HNO₃.

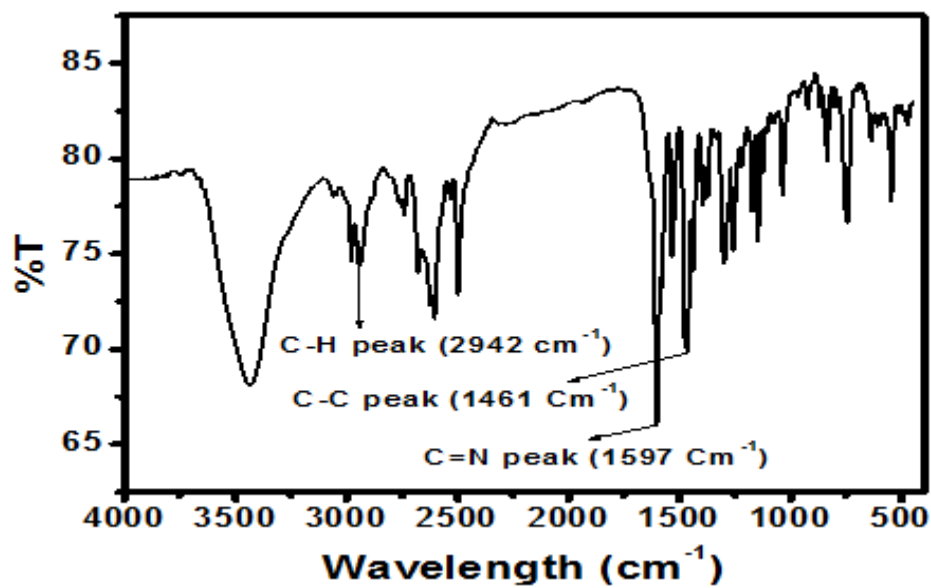


Figure S6. FTIR spectrum of pure sample of Mn-HBAP.

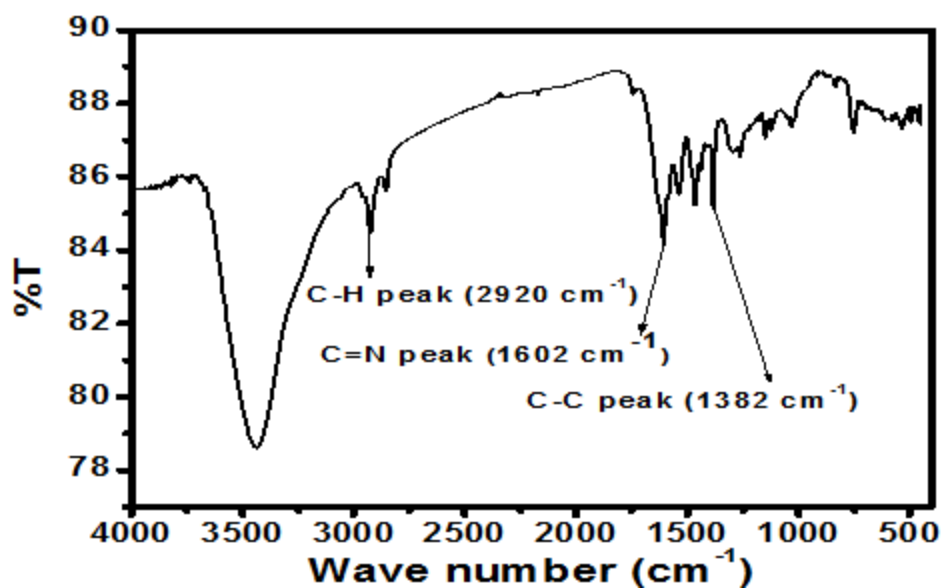


Figure S7. FTIR spectrum of corrosion product of chrome steel in the presence of Mn-HBAP.

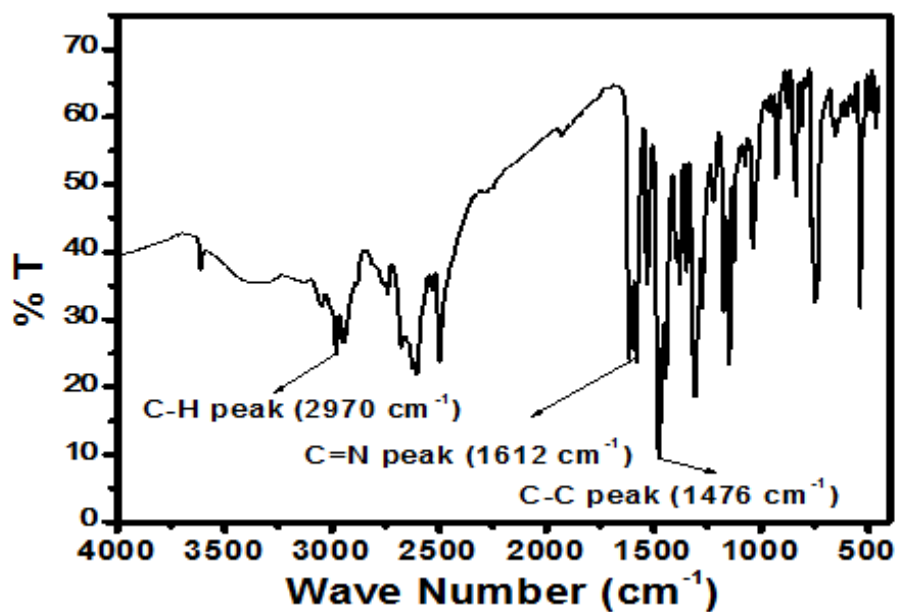


Figure S8. FTIR spectrum of pure sample of Co-HBAP.

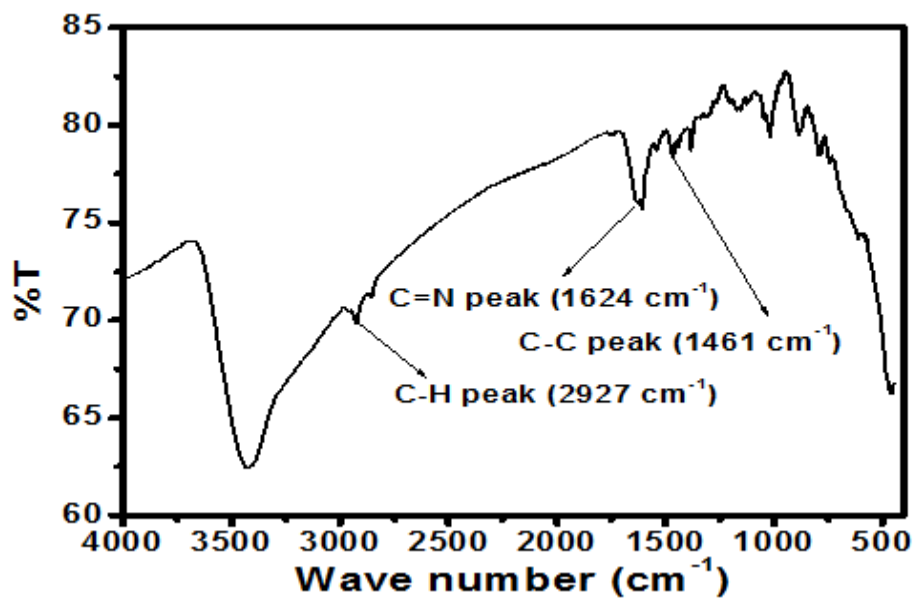
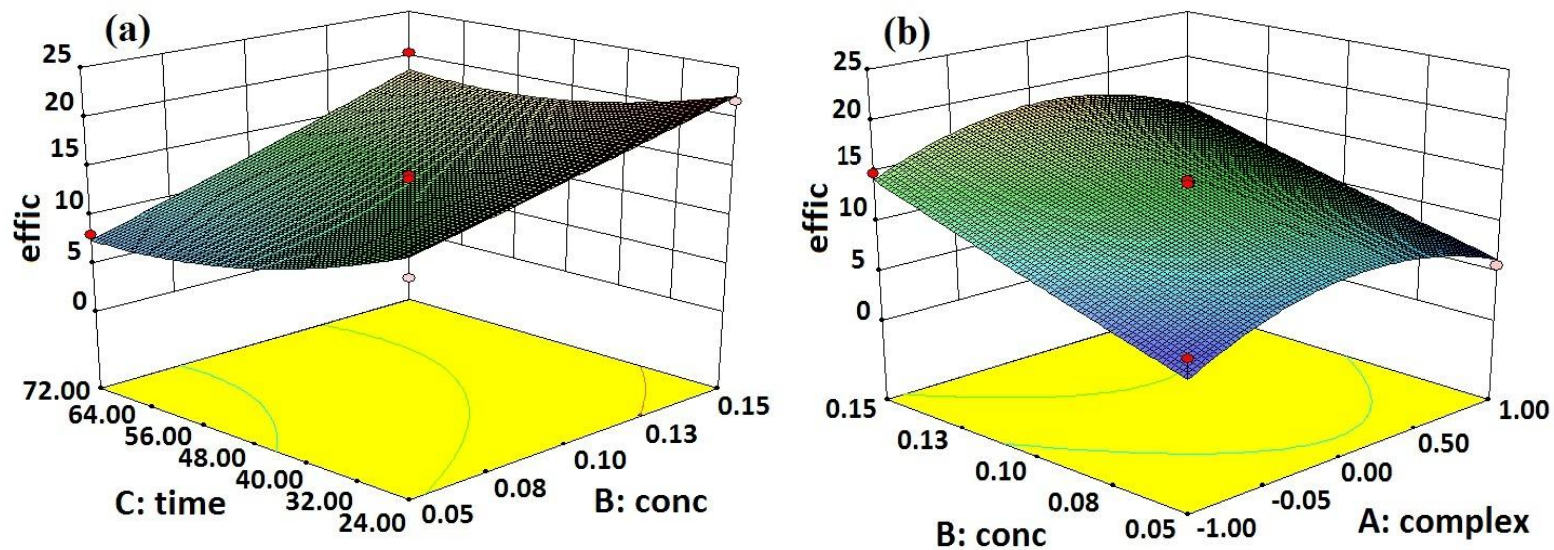


Figure S9. FTIR spectrum of corrosion product of chrome steel in the presence of Co-HBAP.



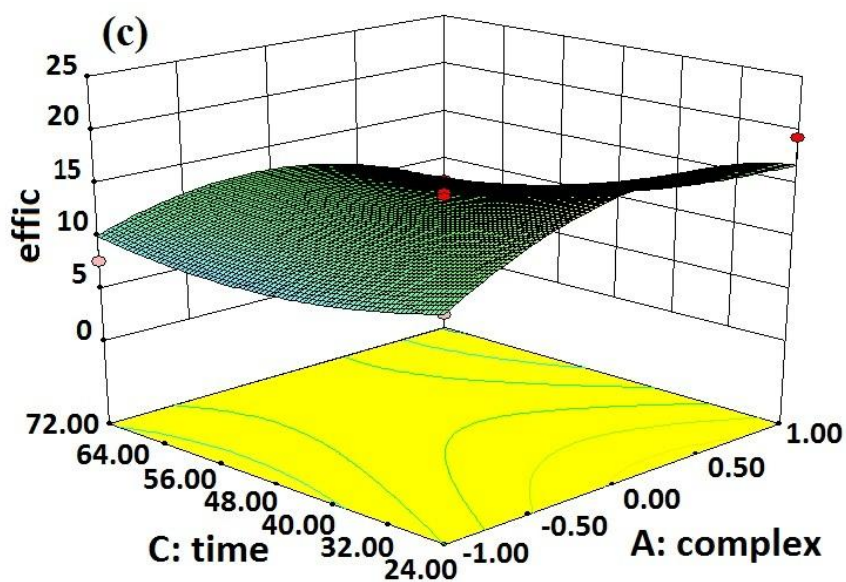


Figure S10. (a) 3D plot of efficiency at different concentration and time, (b) 3D plot of efficiency for different complex and its concentration and (c) 3D plot of efficiency for different complex and time.

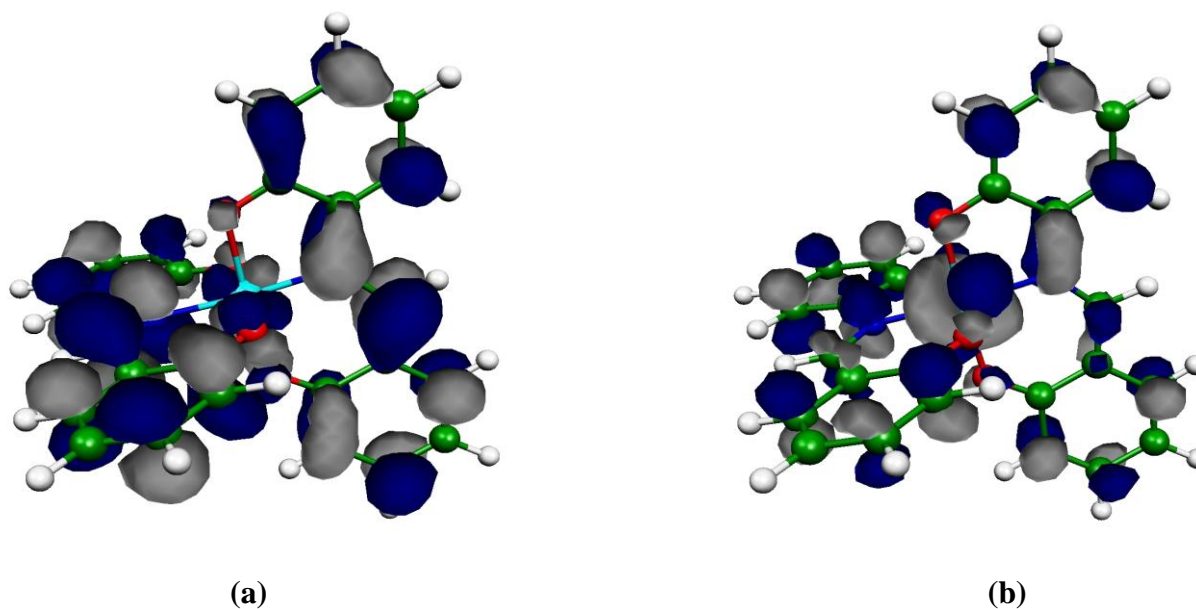


Figure S11. DFT-derived Mulliken Spin Density Plot of UCO orbitals of Mn-HBAP complex (a) HOMO and (b) LUMO plot of Mn-HBAP complex

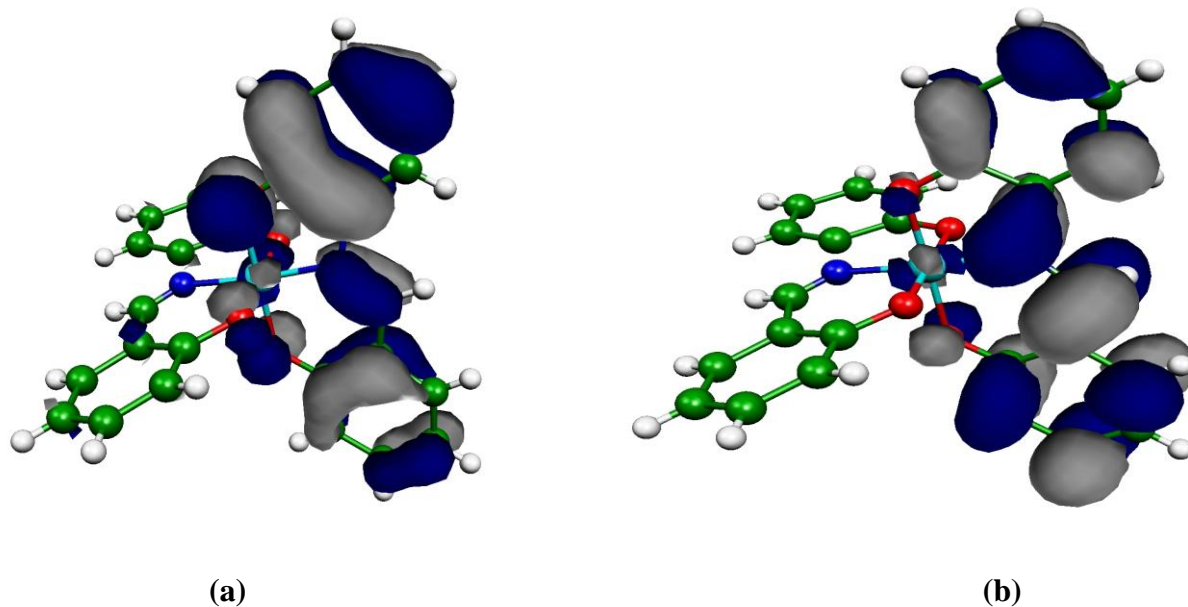


Figure S12. DFT-derived Mulliken Spin Density Plot of UCO orbitals of Co-HBAP complex (a) HOMO and (b) LUMO plot of Co-HBAP complex.